PHYSICAL REVIEW B **93**, 104508 (2016)

Correlation of superconductivity with crystal structure in $(NH_3)_yCs_xFeSe$

Lu Zheng,[1] Xiao Miao,[1] Yusuke Sakai,[1] Hidenori Goto,[1] Eri Uesugi,[1] Ritsuko Eguchi,[1] Saki Nishiyama,[1] Kunihisa Sugimoto,[2] Akihiko Fujiwara,[3] and Yoshihiro Kubozono[1,4,*]

[1]*Research Laboratory for Surface Science, Okayama University, Okayama 700-8530, Japan*
[2]*Japan Synchrotron Radiation Research Institute, SPring-8, Hyogo 679-5198, Japan*
[3]*Department of Nanotechnology for Sustainable Energy, Kwansei Gakuin University, Sanda 669-1337, Japan*
[4]*Research Centre of New Functional Materials for Energy Production, Storage and Transport, Okayama University, Okayama 700-8530, Japan*

(Received 7 October 2015; revised manuscript received 9 January 2016; published 8 March 2016)

The superconducting transition temperature T_c of ammoniated metal-doped FeSe $(NH_3)_yM_xFeSe$ (M: metal atom) has been scaled with the FeSe plane spacing, and it has been suggested that the FeSe plane spacing depends on the location of metal atoms in $(NH_3)_yM_xFeSe$ crystals. Although the crystal structure of $(NH_3)_yLi_xFeSe$ exhibiting a high T_c (~44 K) was determined from neutron diffraction, the structure of $(NH_3)_yM_xFeSe$ exhibiting a low T_c (~32 K) has not been determined thus far. Here, we determined the crystal structure of $(NH_3)_yCs_{0.4}FeSe$ ($T_c = 33$ K) through the Rietveld refinement of the x-ray diffraction (XRD) pattern measured with synchrotron radiation at 30 K. The XRD pattern was analyzed based on two different models, on-center and off-center, under a space group of $I4/mmm$. In the on-center structure, the Cs occupies the 2*a* site and the N of NH_3 may occupy either the 4*c* or 2*b* site, or both. In the off-center structure, the Cs may occupy either the 4*c* or 2*b* site, or both, while the N occupies the 2*a* site. Only an on-center structure model in which the Cs occupies the 2*a* and the N of NH_3 occupies the 4*c* site provided reasonable results in the Rietveld analysis. Consequently, we concluded that $(NH_3)_yCs_{0.4}FeSe$ can be assigned to the on-center structure, which produces a smaller FeSe plane spacing leading to the lower T_c.

DOI: 10.1103/PhysRevB.93.104508

I. INTRODUCTION

The study on metal-doped FeSe is one of the most exciting research subjects because its superconducting transition temperature (T_c) has reached a value greater than 45 K [1–4]. Metal-doped FeSe materials can be synthesized using the high-temperature-annealing method [1,5–8] and liquid-ammonia technique [2,3,9–14], and its T_c can be increased by increasing the FeSe plane spacing [2,4]. On the other hand, it was found that pressure application resulted in a high-T_c phase with the T_c reaching a value greater than 45 K [1,2]. Currently, the highest T_c reported in bulk superconductors of metal-doped FeSe is 49 K at 21 GPa [2]. Even at ambient pressure, the T_c of ammoniated metal-doped FeSe materials has reached 46 K for $(NH_3)_yNa_{0.5}FeSe$ [3]. The insertion of NH_3 molecules or ammoniated metal coordinates between the FeSe layers in metal-doped FeSe can increase the FeSe plane spacing to produce a higher T_c. From the analogy with the relation between the T_c and interlayer distance in ZrNCl [15] and HfNCl [16], we believe that increasing the lattice constant c (or FeSe plane spacing) increases two-dimensionality (2D) to improve Fermi-surface nesting, which enhances spin fluctuation to reinforce the superconducting pairing interaction [2].

Here, it is important to note that the ionic radius of the metal atom inversely correlates with the T_c [11] because metal atoms such as Rb and Cs with larger ionic radii lead to a smaller FeSe plane spacing and, in turn, lower T_c. Our studies on the relationship between c and T_c in $(NH_3)_yM_xFeSe$ clarified that the T_c could be directly scaled with the FeSe plane spacing [2,11]. Therefore, we must investigate the reason why the metal atoms with smaller ionic radius can produce higher FeSe plane spacing. Our previous study on $(NH_3)_yNa_xFeSe$ exhibiting different T_c's, 32 and 46 K [3,12,17], suggested that a difference in the location of metal atoms in each phase resulted in a different FeSe plane spacing, leading to a different T_c. This was suggested from the analogy of the FeSe plane spacing and T_c of the high-T_c ($T_c = 46$ K [3,14]) phase in $(NH_3)_yNa_xFeSe$ with those of $(NH_3)_yLi_xFeSe$ ($T_c = 44$ K [3,10]), while the FeSe plane spacing and T_c of the low-T_c phase ($T_c = 32$K [12,17]) with those of K_xFeSe ($T_c = 31$ K [5]). The Rietveld refinement of the neutron diffraction of $(NH_3)_yLi_xFeSe$ clarified that the Li occupied the 4*c* and 2*b* sites and the N of NH_3 occupied the 2*a* site [10]. We call this structure the off-center structure because the Li atom is not located in the 2*a* site (0,0,0). On the other hand, we call the structure of K_xFeSe the on-center structure because the K atom occupies the 2*a* site [5]. We previously reported the crystal structure of $(NH_3)_yCs_xFeSe$ [11] in which the Cs atom occupied the 2*a* site, i.e., the on-center structure, but the NH_3 was not included in the analysis. Therefore, a detailed structural analysis for $(NH_3)_yCs_xFeSe$ is indispensable to confirm the scenario in which a metal atom with large ionic radius occupies the 2*a* site.

In this paper, we measured the x-ray diffraction (XRD) patterns of $(NH_3)_yCs_{0.4}FeSe$ at different temperatures, and Le Bail fitting was performed to determine the temperature dependence of lattice constants. Furthermore, the Rietveld refinement of the XRD pattern at 30 K was performed using two different models representing the on-center and off-center structures under a space group of $I4/mmm$. Only a Rietveld analysis based on the on-center model provided a reasonable crystal structure, showing that the Cs atom occupied the 2*a* site

*kubozono@cc.okayama-u.ac.jp

and the N of NH_3 occupied the 4*c* site. The chemical composition was determined to be $(NH_3)_{0.37(4)}Cs_{0.268(4)}FeSe$. In the analysis, a deficiency of Fe was not observed. Furthermore, we investigated the x dependence of T_c in $(NH_3)_yCs_xFeSe$ and discussed the constant T_c value observed from view of the structure.

II. EXPERIMENTAL

The β-FeSe sample was prepared using the annealing method described in Ref. [11]. The sample of $(NH_3)_yCs_xFeSe$ was synthesized using the liquid-NH_3 technique described in Ref. [11] with a nominal $x = 0.4$. The experimental procedure is the same as that in our previous reports [2,11]. The dc magnetic susceptibilities M/H's, of all samples were measured using a superconducting quantum interference device (SQUID) magnetometer (Quantum Design MPMS2); here, M and H refer to the magnetization and applied magnetic field, respectively. The M/H in this paper corresponds to the mass magnetic susceptibility ($cm^3\ g^{-1} = emu\ g^{-1}$). The XRD pattern of the sample was measured with synchrotron radiation (wavelength $\lambda = 0.400176(2)$ Å) in BL02B2 of SPring-8, Japan. The sample was introduced into a quartz tube and a capillary for M/H measurement and XRD, respectively, in an Ar-filled glove box (H_2O, $O_2 < 0.1$ ppm); the capillary was filled with He gas. Le Bail and Rietveld refinements were performed using the GSAS program.

III. RESULTS AND DISCUSSION

Figure 1(a) shows the temperature dependence of magnetic susceptibility (M/H in $cm^3\ g^{-1}$) at zero-field cooling (ZFC) and field cooling (FC) for the $(NH_3)_yCs_{0.4}FeSe$ sample. The onset superconducting transition temperature (T_c^{onset}) and T_c were determined to be 35 and 33.5 K, respectively, from the $M/H - T$ plots. As shown in the inset of Fig. 1(a), the T_c is determined from the cross point of the drop of M/H and the extrapolation of the normal state. The shielding fraction of the sample was 25% at 10 K. The $M/H - T$ plots suggest the presence of pure β-FeSe, which exhibits a T_c as high as 8 K.

Figure 1(b) shows the XRD patterns measured at different temperatures. These patterns suggest that the crystal structure is the same in the entire temperature range, i.e., no structural phase transition occurs. The Le Bail fitting of the XRD pattern at 30 K is shown in Fig. 1(c). The Le Bail fitting was achieved assuming the presence of three different crystal phases: $(NH_3)_yCs_xFeSe$, β-FeSe, and α-FeSe. The XRD pattern consists of the overlapped peaks from three phases, but some peaks can be assigned to only a single phase among three phases, indicating the presence of three phases. Thus,

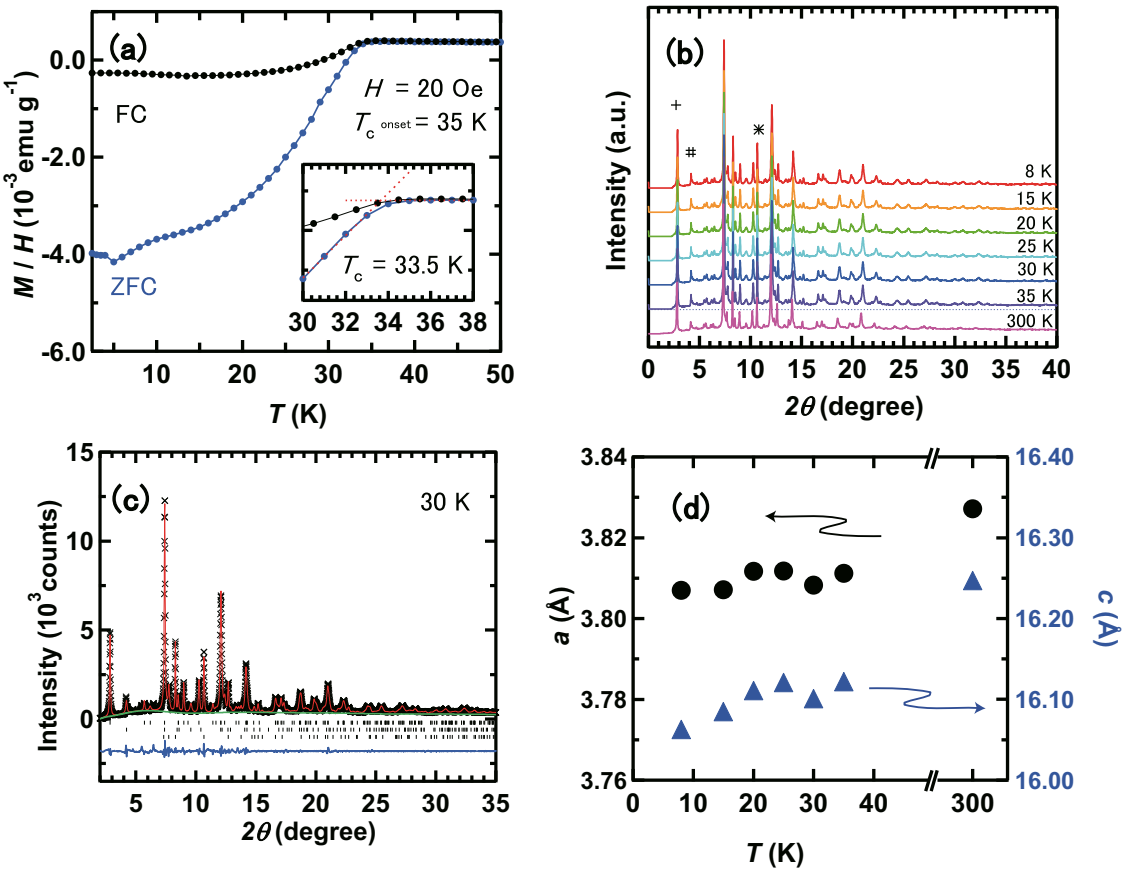

FIG. 1. (a) M/H versus T plots and (b) temperature-dependent XRD patterns of $(NH_3)_yCs_{0.4}FeSe$. In (b), the peaks due to only a single phase among three phases of $(NH_3)_yCs_{0.4}FeSe$, β-FeSe, and α-FeSe are shown by symbols +, #, and ∗, respectively. (c) Le Bail fitting curve (red line) and experimental XRD pattern (x mark) of $(NH_3)_yCs_{0.4}FeSe$ at 30 K. Ticks indicate the positions of Bragg reflections predicted from the lattice constants suggested for $(NH_3)_yCs_{0.4}FeSe$ (top), β-FeSe (middle), and α-FeSe (bottom). The difference between the Le Bail fitting and experimental XRD is indicated in blue. (d) Lattice constants a and c are plotted as a function of T.

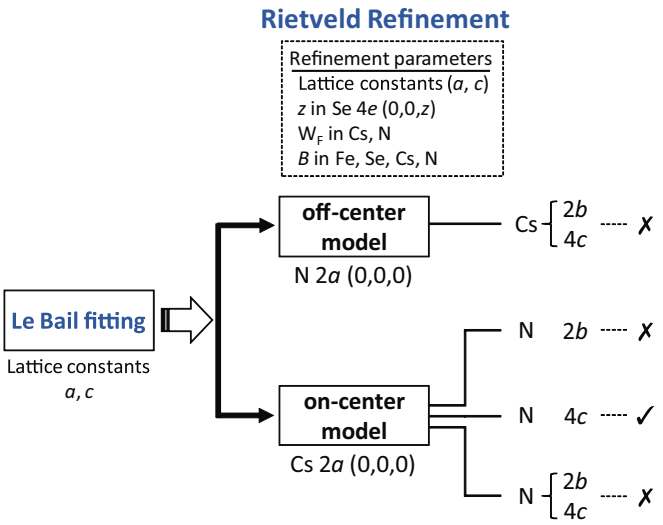

FIG. 2. Process of Rietveld refinement for the XRD pattern measured at 30 K for $(NH_3)_yCs_{0.4}FeSe$.

the XRD pattern could be well analyzed considering the above three phases.

We determined the lattice constants for these crystal phases based on previous reports; the space groups for $(NH_3)_yCs_xFeSe$, β-FeSe, and α-FeSe were $I4/mmm$ (#139) [5,10,11,14], $P4/nmm$ (#129) [11,18,19], and $P6_3/mmc$ (#94) [11,20], respectively. The lattice constants a and c were determined to be 3.8082(2) and 16.097(1) Å, respectively, for $(NH_3)_yCs_xFeSe$, 3.7739(3) and 5.4417(9) Å for β-FeSe, and 3.6166(1) and 5.9233(4) Å for α-FeSe, respectively.

Figure 1(d) shows the temperature dependence of the a and c of $(NH_3)_yCs_{0.4}FeSe$. The a and c at 300 K for $(NH_3)_yCs_{0.4}FeSe$ were determined to be 3.8272(2) and 16.243(1) Å, respectively, which are the same as those, 3.8331(1) and 16.217(1) Å, determined previously by our group [11]. The ratio of lattice constants at 8 K with respect to those at 300 K, a(8 K)/a(300 K) and c(8 K)/c(300 K), were 0.994 and 0.989, respectively, suggesting a slightly larger thermal shrinkage along the c direction consisting of van der Waals interaction between FeSe layers.

Next, we discuss the Rietveld analysis of the XRD pattern of the $(NH_3)_yCs_{0.4}FeSe$ sample at 30 K. The strategy for the Rietveld analysis is schematically shown in Fig. 2. To investigate the validity of the models, the Rietveld analyses were performed using two models (on-center and off-center). In the analysis, the three phases, $(NH_3)_yCs_xFeSe$, β-FeSe, and α-FeSe, were included, in the same manner as in the Le Bail fitting [Fig. 1(c)], and the space groups of $I4/mmm$, $P4/nmm$, and $P6_3/mmc$ were adopted, respectively. In all analyses, the structures of β-FeSe and α-FeSe were taken from previous reports [11,18,19,20]. The Fe and Se of $(NH_3)_yCs_xFeSe$ were located at the 4d and 4e sites, respectively, which are the same as their location in non-ammoniated K_xFeSe [5].

As shown in Fig. 2, in the off-center model, the Cs atoms in $(NH_3)_yCs_xFeSe$ are located at the 4c (0, 1/2, 0) and 2b (0, 0, 1/2) sites, and the N of NH_3 was located at the 2a site (0, 0, 0); the structure is the same as that of $(NH_3)_yLi_xFeSe$ [10]. The H atom was not included in the analysis throughout this study. The occupancy of Cs and N were refined, while the occupancy of Fe and Se were fixed to 1.0. The Debye-Waller factor B ($B = 8\pi^2U$, U: isotropic thermal-displacement of atom) for all atoms (Fe, Se, Cs, and N) were refined in the $(NH_3)_yCs_xFeSe$ phase, and z at the 4e site (Se) were refined. The refinements of β-FeSe and α-FeSe were performed together with that of $(NH_3)_yCs_xFeSe$. In β-FeSe, the Fe and Se atoms were located at 2a (3/4, 1/4, 0) and 2c (1/4, 1/4, z) sites (choice #2 of $P4/nmm$), respectively, and the z at the 2c site and B values at both sites were refined; occupancies at both sites were fixed to 1.0. In α-FeSe, the Fe and Se atoms were located at the 2a (0, 0, 0) and 2c (1/3, 2/3, 1/4) sites, respectively, and the B values at both sites were refined. The lattice constants of three phases were refined together with background and peak-shape (profile-function) parameters; CW profile function 2 of the GSAS program was used for the profile function. This function employs a multiterm Simpson's rule integration of the pseudo-Voigt function [21]. The parameters of profile functions are refined independently for each phase.

In the refinement with the off-center model described above, the fractions of $(NH_3)_yCs_xFeSe$, β-FeSe, and α-FeSe were evaluated to be 37, 33, and 30%, respectively. The a and c of $(NH_3)_yCs_xFeSe$ were determined to be 3.8050(3) and 16.066(2) Å, respectively, which are almost the same as those, 3.8082(2) and 16.097(1) Å, evaluated from the Le Bail fitting [Fig. 1(c)]. However, the B of the Cs at the 4c site rapidly increased to 63(12) Å^2, while the B of the Cs at the 2b site had a negative value. Furthermore, the occupancy of N diverged. As a reference, the XRD pattern calculated based on the off-center structure of the $(NH_3)_yCs_xFeSe$ phase and the structures of β-FeSe and α-FeSe is shown in Fig. 3(a), together with the experimental XRD pattern; the weighted R factor (wR_p) and pattern R factor (R_p) were 11.3 and 7.7%, respectively. From the unreasonable B factors and occupancy, we must conclude that this refinement is not successful, showing that the off-center model cannot be applied for the $(NH_3)_yCs_xFeSe$ phase. The logarithmic scale of the experimental XRD pattern is shown together with the logarithmic-scaled pattern calculated (off-center model) in Fig. 3(b), to clearly show the entire XRD pattern.

As shown in Fig. 2, we subsequently analyzed the XRD pattern based on the on-center model (space group: $I4/mmm$) for $(NH_3)_yCs_xFeSe$. In the same manner as the analysis based on the off-center model for $(NH_3)_yCs_xFeSe$, β-FeSe and α-FeSe were included in the analysis. The structures of β-FeSe and α-FeSe are the same as those used in the off-center structure analysis. The lattice constants of three phases were refined together with the background, and the parameters of the profile function were independently refined for each phase; the profile function is the same as that in the off-center model.

In the $(NH_3)_yCs_xFeSe$ phase, the Cs atom was located at the 2a (0, 0, 0) site, while the N atom of NH_3 was located at the 2b (0, 0, 1/2) site. The occupancy of Cs and N were refined, while the occupancy of Fe and Se were fixed to 1.0. The B values for all elements and z at the 4e site were refined in the $(NH_3)_yCs_xFeSe$ phase. The Rietveld refinement showed a negative occupancy and negative B for the N atom (2b site), indicating that this structure (on-center model) can also be ruled out for the $(NH_3)_yCs_xFeSe$ phase.

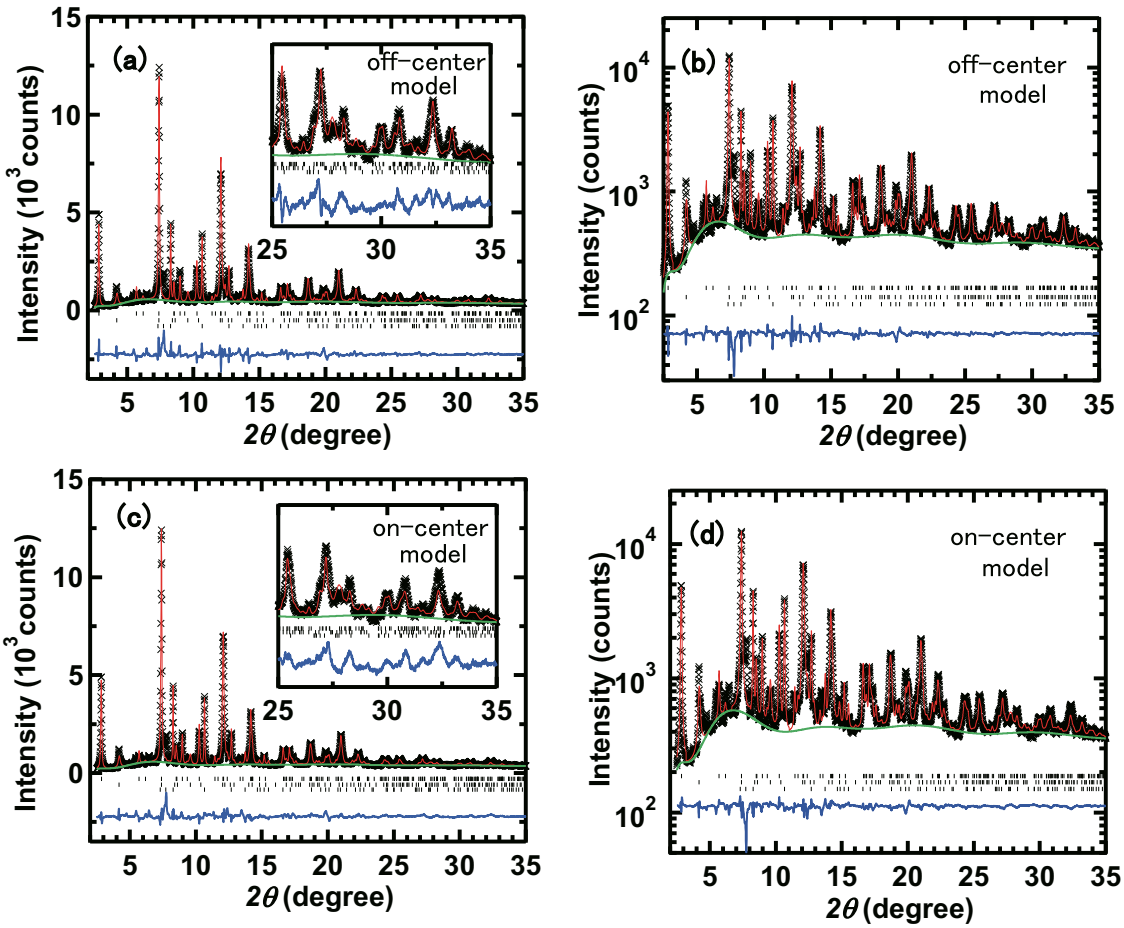

FIG. 3. Curves (red line) calculated using the Rietveld refinement and the experimental XRD pattern (x mark) of $(NH_3)_yCs_{0.4}FeSe$ at 30 K. Rietveld refinement was achieved based on (a) the off-center model and (c) the on-center model. Ticks indicate the positions of Bragg reflections predicted from the lattice constants suggested for $(NH_3)_yCs_{0.4}FeSe$ (top), β-FeSe (middle), and α-FeSe (bottom). The difference between the calculated and experimental XRD patterns is indicated in blue. In the inset of (a) and (c), the calculated and experimental XRD pattern (expanded) in high 2θ angle is shown. The logarithmic scale of the experimental XRD pattern and the logarithmic-scaled pattern calculated using (b) the off-center and (d) the on-center models.

Next, in the on-center model, the N atom was moved to the $4c$ $(0,1/2,0)$ site from the $2b$ site. The occupancy of Cs and N, B values of all elements, and z of the $4e$ site were refined in this analysis. This analysis successfully provided reasonable values for occupancy, B, and z, as listed in Table I. The a and c for $(NH_3)_yCs_xFeSe$ were 3.8075(2) and 16.048(2) Å, respectively, which are the same as those [3.8082(2) and 16.097(1) Å] at 30 K obtained using Le Bail fitting [Fig. 1(d)]. The refined structures of β-FeSe and α-FeSe are also reasonable (see Table I). Consequently, the on-center structure in which the Cs occupies the $2a$ site and the N occupies the $4c$ site was identified for $(NH_3)_yCs_xFeSe$. From the determined occupancies of N and Cs, the chemical stoichiometry was evaluated to be $(NH_3)_{0.37(4)}Cs_{0.268(4)}FeSe$. The x value [0.268(4)] determined from the occupancy of Cs at the $2a$ site was consistent with that [$x = 0.255(5)$] reported previously for the other batch of $(NH_3)_yCs_xFeSe$ (nominal $x = 0.4$) [11] and was almost consistent with the nominal x value (=0.4), indicating a reliable occupancy. However, it should be recognized that the occupancy is evaluated under the restriction of $I4/mmm$ symmetry.

The fractions of $(NH_3)_yCs_xFeSe$, β-FeSe, and α-FeSe were 36, 34, and 32%, respectively. The wR_p and R_p were 10.7 and 7.1%, respectively, indicating a better analysis with the on-center model than the off-center model. The calculated XRD pattern is shown in Fig. 3(c), together with the experimental XRD pattern, and the logarithmic scale of the experimental XRD pattern is shown together with the calculated pattern in Fig. 3(d), to clearly show the entire experimental and calculated XRD patterns.

To confirm the on-center structure (Cs: $2a$ site, N: $4c$ site), the N atom was assumed at both the $2b$ and $4c$ sites, and refinement was performed. Consequently, the occupancy for the N at the $2b$ site vanished, and that for the N at the $4c$ site had the same value as that in the analysis based on the on-center model (Cs: $2a$ site, N: $4c$ site) described above. The B values of N at the $2b$ and $4c$ sites provided negative and reasonable values, respectively. These results imply that the N does not exist at the $2b$ site; rather, it exists at the $4c$ site. Thus, our analysis of the XRD pattern of the $(NH_3)_yCs_{0.4}FeSe$ sample successfully resulted in the on-center structure (Cs: $2a$ site, N: $4c$ site) for the $(NH_3)_yCs_xFeSe$

TABLE I. Final crystal structure of $(NH_3)_yCs_{0.4}FeSe$ determined using Rietveld refinement.

1) Phase 1. $(NH_3)_yCs_{0.4}FeSe$
Body-centered tetragonal lattice: $I4/mmm$ (No. 139)
Volume fraction: 35.8%
Lattice constants: $a = 3.8075(2)$ Å, $c = 16.048(2)$ Å

		Occupancy	x	y	z	B(Å^2)
4d	Fe	1.0	0.00000	0.50000	0.25000	0.2(1)
4e	Se	1.0	0.00000	0.00000	0.3436(2)	0.56(7)
2a	Cs	0.535(7)	0.00000	0.00000	0.00000	2.1(2)
4c	N	0.37(4)	0.00000	0.50000	0.00000	12(3)

2) Phase 2. β-FeSe
Tetragonal lattice: $P4/nmm$ (No. 129, choice 2)
Volume fraction: 33.5%
Lattice constant: $a = 3.7666(8)$, $c = 5.458(2)$ Å

		Occupancy	x	y	z	B(Å^2)
2a	Fe	1.0	0.75000	0.25000	0.00000	1.2(3)
2c	Se	1.0	0.25000	0.25000	0.266(1)	1.4(2)

3) Phase 3. α-FeSe
Hexagonal structure: $P6_3/mmc$ (No. 194)
Volume fraction: 31.6%
Lattice constant: $a = 3.6166(3)$ Å, $c = 5.9293(8)$ Å

		Occupancy	x	y	z	B(Å^2)
2a	Fe	1.0	0.00000	0.00000	0.00000	1.5(2)
2c	Se	1.0	0.33333	0.66667	0.25000	0.7(1)

phase. The structure suggested for $(NH_3)_yCs_xFeSe$ is shown in Fig. 4(a). Here, we must comment that the fraction of 36% determined from the Rietveld refinement is a little different from the shielding fraction (∼25%) from the magnetic susceptibility. Such a deviation is also found in the previous report [11]. One possibility for the lower volume fraction (∼25%) determined from magnetic susceptibility is that the presence of nonsuperconducting/magnetic α-FeSe may suppress the superconducting state. At the present stage, the origin remains to be clarified.

We attempted to determine the occupancy of Fe in the $(NH_3)_yCs_xFeSe$ phase. In the final structure [Table I and Fig. 4(a)], only the occupancy and B of Fe (4d site) were refined to determine the deficiency of Fe, providing the chemical

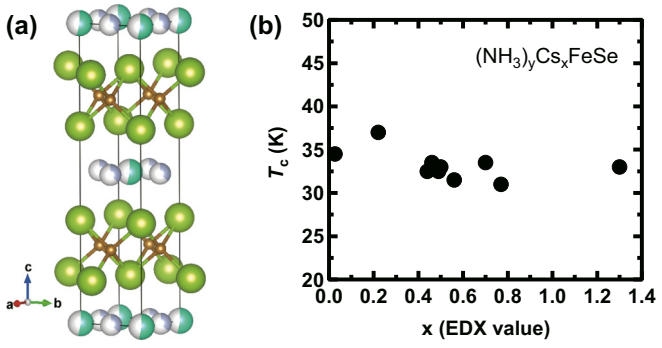

FIG. 4. (a) Schematic crystal structure of $(NH_3)_yCs_{0.4}FeSe$ ultimately determined using the Rietveld refinement. This structure corresponds to the on-center structure. (b) x dependence of T_c in $(NH_3)_yCs_{0.4}FeSe$.

stoichiometry of $(NH_3)_{0.37(4)}Cs_{0.268(4)}Fe_{0.989(4)}Se$. This implies the absence of a deficiency of Fe in $(NH_3)_yCs_xFeSe$, which is reasonable from the low paramagnetic susceptibility observed in the normal state [Fig. 1(a)]. Finally, we calculated the difference Fourier map using the on-center model structure (Cs: 2a site, N: 4c site), which refers to electron density distribution evaluated from the difference between the XRD observed and that calculated with the on-center model. No electron densities were observed at the 2a and 4c sites, showing clearly that the above on-center model is reasonable. In addition, the electron density was observed at the 2a site in the difference Fourier map when the N atom was located at the 2a site (off-center model), indicating the electrons are inefficient, i.e., the element is not N but Cs at 2a site. This supports the validity of the on-center model.

We tried to determine the anisotropic thermal displacements U_{ij}'s for Fe, Se, Cs, and N. However, the anisotropic thermal parameters could not be shown since complete analyses have not been achieved, probably because of an insufficient data quality. Nevertheless, if we shortly comment, the anisotropic parameters U_{11}, U_{22}, and U_{33} of N and Cs became negative in the off-center model, while those were positive in the on-center model, indicating that the on-center model is suitable.

Furthermore, we evaluated the particle size from 002 reflection, which refers to the particle size along the c axis. The particle size along the a axis could not be obtained because all peaks ascribable to h 00 reflection were overlapped from peaks due to other indices. Therefore, we could not compare the particle size between the a and c axes. The particle size (=27 nm) along the c axis seems to be a little small, but it is still unclear whether the small particle size originates from the 2D of $(NH_3)_yCs_xFeSe$.

The present structure analysis for $(NH_3)_yCs_xFeSe$ and the previous one for $(NH_3)_yLi_xFeSe$ using neutron diffraction [10] show that the positions of the metal atom and N atom are different between Cs and Li. The c, 16.5266(9) Å, of $(ND_{2.8(1)})_{0.5}Li_{0.30(5)}FeSe$ (off-center structure) [10] is larger than that, 16.243(1) Å, of $(NH_3)_{0.37(4)}Cs_{0.268(4)}FeSe$ (on-center structure) determined using Le Bail fitting at 300 K, indicating that the off-center structure leads to an increased FeSe plane spacing, which produces higher T_c because of the increase in the 2D. Table II lists the interatomic distances determined with the on-center and off-center models. The interatomic distances can be compared with those in $(NH_3)_yLi_xFeSe$ and K_xFeSe reported previously [5,10]. The interatomic distances determined from the off-center model are consistent with those of the previous report on $(NH_3)_yLi_xFeSe$ (off-center structure) [5]. On the other hand, the interatomic distances in the on-center model could not be compared directly with those of other $(NH_3)_yM_xFeSe$ having on-center structure because of no data, but as seen from Table II, the Fe-Se and M-Se distances are consistent with those of non-ammoniated K_xFeSe (on-center structure), indicating that the analysis based on the on-center model is reliable.

Here, it is worth noting that the limited x in $(NH_3)_yM_xFeSe$ is 0.5 for the on-center structure since the M occupies the 2a site, while it increases to 1.5 for the off-center structure since the M can occupy the 2b and 4c sites. Since the x in $(NH_3)_yCs_xFeSe$ and $(NH_3)_yLi_xFeSe$, as described above, is less than 0.5, they can have both the on-center and

TABLE II. Selected interatomic distances and angles in the off-center and on-center models for $(NH_3)_yCs_xFeSe$ and those in $(NH_3)_yLi_xFeSe$ (off-center structure) and K_xFeSe (on-center structure). The site where each element occupies is also shown.

	Off-center model	On-center model	$(NH_3)_yLi_xFeSe$[a]	K_xFeSe[b]
Fe-Se (Å)	2.4074(2)	2.4229(1)	2.408(1)	2.4406(4)
	4*d*-4*e*	4*d*-4*e*	4*d*-4*e*	4*d*-4*e*
Se-Fe-Se (Å)	104.4217(1)	103.5818(1)	104.40(8)	106.600(4)
	4*d*-4*e*-4*d*	4*d*-4*e*-4*d*	4*d*-4*e*-4*d*	4*d*-4*e*-4*d*
M-N (Å)	1.9025(1)	1.9038(1)	1.9029(1)	No
	4*c*-2*a*	2*a*-4*c*	4*c*-2*a*	
M-N (Å)	2.6905(1)	No	2.6912(1)	No
	2*b*-2*a*		2*b*-2*a*	
N-Se (Å)	3.7010 (3)	3.1523(3)	3.7207(1)	No
	2*a*-4*e*	2*a*-4*e*	2*a*-4*e*	
M-Se (Å)	3.1746(3)	3.6828(2)	3.1972(1)	3.4443(4)
	4*c*-4*e*	2*a*-4*e*	4*c*-4*e*	2*a*-4*e*
M-Se (Å)	2.5414(4)	No	2.5693(1)	No
	2*b*-4*e*		2*b*-4*e*	

[a]Taken from Ref. [10].
[b]Taken from Ref. [5].

off-center structures. Actually, depending on the ionic radius, the structure adopted seems to be different. Our recent paper showed that $(NH_3)_yNa_xFeSe$ has two superconducting phases ($T_c = 32$ K and 46 K [17]) depending on the x value, and the phases have different c values [14.145(8) Å for the 32 K phase and 17.565(7) Å for the 46 K phase]. A value of x greater than 0.5 produces the high-T_c phase, presumably owing to the off-center structure, which is reasonable because a value of x greater than 0.5 is not allowed for the on-center structure. Furthermore, our paper showed that $(NH_3)_yLi_xFeSe$ possessed only a single superconducting phase when varying x [17]. Therefore, the x dependence of T_c in $(NH_3)_yCs_xFeSe$ is of interest because it would directly relate to whether the position of the Cs atom varies with x.

The x dependence of T_c showed that the T_c did not change when varying the nominal x value from 0.0 to 1.3 [Fig. 4(b)], and it was constant at 33 ± 2 K. This indicates that only an on-center structure is adopted in $(NH_3)_yCs_{0.4}FeSe$, and the Cs amount intercalated in the FeSe lattice may be $x \leqslant 0.5$ despite varying the x value. Only a single phase ($T_c \sim 33$K) was realized in $(NH_3)_yCs_xFeSe$, which is different from $(NH_3)_yNa_xFeSe$ and $(NH_3)_yLi_xFeSe$, indicating the ionic radius of the intercalant is a key for determining the T_c, i.e., the larger ionic radius leads to the lower T_c.

IV. CONCLUSIONS

The Rietveld refinement of the XRD pattern of $(NH_3)_yCs_{0.4}FeSe$ was successfully achieved, and it revealed an on-center structure in which the Cs and the N of NH_3 occupy the 2*a* and 4*c* sites, respectively. This suggests that the low-T_c phase ($T_c \sim 32$ K) found in $(NH_3)_yM_xFeSe$ takes the on-center structure, while the high-T_c phase ($T_c \sim 45$ K) takes the off-center structure, as determined for $(NH_3)_yLi_xFeSe$ [10]. The on-center structure has a smaller FeSe plane spacing than that of the off-center structure, and the FeSe plane spacing closely relates to the T_c. This paper clarified not only the structural difference between the low-T_c and high-T_c phases in $(NH_3)_yM_xFeSe$, but also the effect of the location of the metal and NH_3 atoms on the FeSe plane spacing (or T_c). As the location of metal atoms with relatively large and small ionic radii (Cs and Li) was determined, the next target for determination must be FeSe materials incorporating a metal atom with intermediate ionic radius such as Na, which produces multiple superconducting phases (high-T_c and low-T_c phases [12,17]). This paper constitutes a step towards clarifying the correlation between the crystal structure and T_c in $(NH_3)_yM_xFeSe$.

ACKNOWLEDGMENTS

This study was partly supported by Grants-in-aid No. 22244045, 24654105, and 26105004 from the Ministry of Education, Sports, Science and Technology (MEXT), by the Light Element Molecular Superconductivity (LEMSUPER) project of Strategic International Collaborative Research Program (Japan-EU) in Japan Science and Technology Agency (JST), the Advance Catalytic Transformation Program for Carbon Utilization (ACT-C) in JST, by the Program for Promoting the Enhancement of Research Universities. The x-ray diffraction (XRD) measurement at SPring-8 was performed under the Proposal No. 2014A1102.

[1] L. L. Sun, X.-J. Chen, J. Guo, P. Gao, Q.-Z. Huang, H. Wang, M. Fang, X. Chen, G. Chen, Q. Wu, C. Zhang, D. Gu, X. Dong, L. Wang, K. Yang, A. Li, X. Dai, H. Mao, and Z. Zhao, Nature **483**, 67 (2012).

[2] M. Izumi, L. Zheng, Y. Sakai, H. Goto, M. Sakata, Y. Nakamoto, H. L. Nguyen, T. Kagayama, K. Shimizu, S. Araki, T. C. Kobayashi, T. Kambe, D. Gu, J. Guo, J. Liu, Y. Li, L. Sun, K. Prassides, and Y. Kubozono, Sci. Rep. **5**, 9477 (2015).

[3] T. P. Ying, X. L. Chen, G. Wang, S. F. Jin, T. T. Zhou, X. F. Lai, H. Zhang, and W. Y. Wang, Sci. Rep. **2**, 426 (2012).
[4] T. Noji, T. Hatakeda, S. Hosono, T. Kawamata, M. Kato, and Y. Koike, Physica C **504**, 8 (2014).
[5] J. Guo, S. Jin, G. Wang, S. Wang, K. Zhu, T. Zhou, M. He, and X. Chen, Phys. Rev. B **82**, 180520(R) (2010).
[6] A. F. Wang, J. J. Ying, Y. J. Yan, R. H. Liu, X. G. Luo, Z. Y. Li, X. F. Wang, M. Zhang, G. J. Ye, P. Cheng, Z. J. Xiang, and X. H. Chen, Phys. Rev. B **83**, 060512(R) (2011).
[7] A. Krzton-Maziopa, Z. Shermadini, E. Pomjakushina, V. Pomjakushin, M. Bendele, A. Amato, R. Khasanov, H. Luetkens, and K. Conder, J. Phys.: Condens. Matter **23**, 052203 (2011).
[8] M. Fang, H. Wang, C. Dong, Z. Li, C. Feng, J. Chen, and H. Yuan, Europhys. Lett. **94**, 27009 (2011).
[9] T. Ying, X. Chen, G. Wang, S. Jin, X. Lai, T. Zhou, H. Zhang, S. Shen, and W. Wang, J. Am. Chem. Soc. **135**, 2951 (2013).
[10] M. Burrard-Lucas, D. G. Free, S. J. Sedlmaier, J. D. Wright, S. J. Cassidy, Y. Hara, A. J. Corkett, T. Lancaster, P. J. Baker, S. J. Blundell, and S. J. Clarke, Nat. Mater. **12**, 15 (2013).
[11] L. Zheng, M. Izumi, Y. Sakai, R. Eguchi, H. Goto, Y. Takabayashi, T. Kambe, T. Onji, S. Araki, T. C. Kobayashi, J. Kim, A. Fujiwara, and Y. Kubozono, Phys. Rev. B **88**, 094521 (2013).
[12] Y. Sakai, L. Zheng, M. Izumi, K. Teranishi, R. Eguchi, H. Goto, T. Onji, S. Araki, T. C. Kobayashi, and Y. Kubozono, Phys. Rev. B **89**, 144509 (2014).
[13] S. J. Sedlmaier, S. J. Cassidy, R. G. Morris, M. Drakopoulos, C. Reinhard, S. J. Moorhouse, D. O'Hare, P. Manuel, D. Khalyavin, and S. J. Clarke, J. Am. Chem. Soc. **136**, 630 (2014).
[14] J. G. Guo, H. C. Lei, F. Hayashi, and H. Hosono, Nat. Commun. **5**, 4756 (2014).
[15] S. Yamanaka, J. Mater. Chem. **20**, 2922 (2010).
[16] G. Ye, J. Ying, Y. Yan, X. Luo, P. Cheng, Z. Xiang, A. Wang, and X. Chen, Phys. Rev. B **86**, 134501 (2012).
[17] L. Zheng, X. Miao, Y. Sakai, M. Izumi, H. Goto, S. Nishiyama, E. Uesugi, Y. Kasahara, Y. Iwasa, and Y. Kubozono, Sci. Rep. **5**, 12774 (2015).
[18] F.-C. Hsu, J.-Y. Luo, K.-W. Yeh, T.-K. Chen, T.-W. Huang, P. M. Wu, Y.-C. Lee, Y.-L. Huang, Y.-Y. Chu, D.-C. Yan, and M.-K. Wu, Proc. Natl. Acad. Sci. USA **105**, 14262 (2008).
[19] T. M. McQueen, Q. Huang, V. Ksenofontov, C. Felser, Q. Xu, H. Zandbergen, Y. S. Hor, J. Allred, A. J. Williams, D. Qu, J. Checkelsky, N. P. Ong, and R. J. Cava, Phys. Rev. B **79**, 014522 (2009).
[20] T. Hirone and S. Chiba, J. Phys. Soc. Jpn. **11**, 666 (1956).
[21] C. J. Howard, J. Appl. Cryst. **15**, 615 (1982).